Available online at www.sciencedirect.com
ScienceDirect
International Journal of Solids and Structures 44 (2007) 352–369
INTERNATIONAL JOURNAL OF SOLIDS and STRUCTURES
www.elsevier.com/locate/ijsolstr

Exact resultant equilibrium conditions in the non-linear theory of branching and self-intersecting shells

V. Konopińska, W. Pietraszkiewicz *

Institute of Fluid-Flow Machinery of the Polish Academy of Sciences, ul. Gen. J. Fiszera 14, 80-952 Gdańsk, Poland

Received 30 August 2005; received in revised form 13 April 2006
Available online 29 April 2006

Abstract

We formulate the exact, resultant equilibrium conditions for the non-linear theory of branching and self-intersecting shells. The conditions are derived by performing direct through-the-thickness integration in the global equilibrium conditions of continuum mechanics. At each regular internal and boundary point of the base surface our exact, local equilibrium equations and dynamic boundary conditions are equivalent, as expected, to the ones known in the literature. As the new equilibrium relations we derive the exact, resultant dynamic continuity conditions along the singular surface curve modelling the branching and self-intersection as well as the dynamic conditions at singular points of the surface boundary. All the results do not depend on the size of shell thicknesses, internal through-the-thickness shell structure, material properties, and are valid for an arbitrary deformation of the shell material elements.

Keywords: Shell; Branch; Intersection; Singular curve; Continuity conditions; Exact reduction; Non-linear theory

1. Introduction

Most two-dimensional (2D) models of regular shells known in the literature, such as the Kirchhoff–Love model or the Timoshenko–Reissner model, are formulated using various kinematic constraints on the 3D deformation of the shell material elements. In such shell models the 2D virtual work principle is usually applied to derive approximate equilibrium conditions formulated on the shell base surface.

Reissner (1974, 1982) noted that the non-linear theory of regular shells can be better formulated starting from the resultant 2D equilibrium equations, which can be derived *exactly* by direct through-the-thickness integration of the 3D equilibrium equations of continuum mechanics. The corresponding 2D shell kinematics of the base surface can then be uniquely established as an *energetically exact* dual structure from the virtual work identity. As a result, the gross deformation of a shell cross section is characterised by a translation vector and a rotation tensor that vary on the base surface. The two fields are the only primary variables of the

* Corresponding author. Tel.: +48 58 6995263; fax: +48 58 3416144.
E-mail addresses: violetta@imp.gda.pl (V. Konopińska), pietrasz@imp.gda.pl (W. Pietraszkiewicz).

0020-7683/$ - see front matter © 2006 Elsevier Ltd. All rights reserved.
doi:10.1016/j.ijsolstr.2006.04.030

boundary value problem. Such a general, dynamically and kinematically exact, six-scalar-field theory of regular shells, formulated with regard to a non-material weighted surface of mass taken as the shell base surface, was developed by Libai and Simmonds (1983, 1998) and Simmonds (1984), and with regard to a material surface arbitrary located within the shell-like body by Makowski and Stumpf (1990), Chróścielewski et al. (1992), Pietraszkiewicz (2001a) and Pietraszkiewicz et al. (2005). For this general shell model efficient finite element algorithms were developed and many numerical examples of equilibrium, stability, and dynamics of regular and complex shell structures were presented by Chróścielewski et al. (1992, 1997) and Chróścielewski et al. (2002, 2004).

Many real shell structures contain irregular shell geometry, material properties, loadings, deformations, and/or boundary conditions. The six-field non-linear theory of irregular shell structures was initiated by Makowski and Stumpf (1994) and developed by Chróścielewski et al. (1997), Pietraszkiewicz (2001a), and Chróścielewski et al. (2004). In those works it was assumed that the region of shell irregularity (e.g., branching, self-intersection, stiffening, technological junction, etc.) is small as compared with other shell dimensions and its size can be ignored in deriving the resultant 2D equilibrium conditions. However, such an assumption brings an undefinable error into the resultant dynamic continuity conditions formulated along the singular surface curves modelling the irregularity regions. Therefore, such conditions cannot be regarded as exact implications of 3D equilibrium conditions of continuum mechanics.

In this paper we derive the exact, resultant equilibrium conditions for two important classes of irregular shell structures: the branching shell and the self-intersecting shell. The base surfaces of the irregular shells consist of three and four, respectively, regular material surfaces arbitrary located in the shell space which are joined along the common singular surface curve modelling the junction. The 2D equilibrium conditions are formulated at the base surface by performing direct through-the-thickness integration in the 3D global equilibrium conditions of continuum mechanics. Our through-the-thickness integration procedure is exact and takes into account real dimensions and geometry of the regions of shell branching and self-intersection.

The three regular parts of the branching shell structure are first extended into the junction region up to the singular curve. By this extension some fictitious tractions become applied on four surface strips located at the junction. There are also two tubes within the junction region where the through-the-thickness integration is performed twice. In order to compensate the surplus of forces and couples on the base surface following from the fictitious tractions and the double integration, some statically equivalent system of forces and couples has to be subtracted along the singular curve. As a result of appropriate transformations, our local, resultant equilibrium conditions for the branching shell structure become *exact implications* of the global equilibrium conditions of continuum mechanics. The self-intersecting shell is treated in the same way as the branching shell, only in the former case we have four regular shell parts rigidly connected together at the common junction.

At each regular internal and boundary point of the base surface our exact, local equilibrium equations (30) and dynamic boundary conditions (31) are equivalent, as expected, to the ones given first by Libai and Simmonds (1983). Other two local equilibrium relations – the exact, resultant dynamic continuity conditions (32) along the singular curve and the exact, resultant dynamic boundary conditions (33) at the singular boundary points – are new. They complete the set of resultant equilibrium conditions necessary to appropriately formulate the boundary value problem of the general, six-field theory of branching and self-intersecting shell structures.

Necessary formulae allowing one to express differential volume and surface elements outside the base surface through the corresponding surface elements of the base surface and linear elements of the singular surface curve are given in Appendix. The relations take into account that the rectilinear transverse co-ordinate measuring distance from the base surface may not, in general, be normal to the surface.

2. Notation and preliminary relations

The system of notation used here follows that of Chróścielewski et al. (2004) and Libai and Simmonds (1998).

A shell is a 3D solid body identified in a reference (undeformed) placement with a region B of the physical space $\mathscr{E}$ having the 3D vector space E as its translation space. The shell boundary ∂B consists of three separable parts: the upper M^+ and lower M^- shell faces, and the lateral boundary surface ∂B^* such that $\partial B = M^+ \cup M^- \cup \partial B^*$, $M^+ \cap M^- = \emptyset$.

The position vector $\mathbf{x}$ of any shell point $\mathrm{x} \in B$ can be described by

$$\mathbf{x}(x,\xi) = \boldsymbol{x}(x) + \xi \boldsymbol{t}(x). \tag{1}$$

Here $\boldsymbol{x}(x) = \mathbf{x}(x,0)$ is the position vector of a point x of some reference base surface M arbitrarily located in B, $\xi \in [-h^-(x), h^+(x)]$ is the distance along ξ from M with $h = h^- + h^+ > 0$ the initial shell thickness measured along ξ, and $\boldsymbol{t}(x)$ is the unit vector of the rectilinear co-ordinate line ξ not necessarily normal to M. Such a skew transverse co-ordinate ξ allows one to apply the exact through-the-thickness integration also in case of folded shells or when two shells do not intersect orthogonally, for example. The form (1) requires that the lateral boundary surface ∂B^* be a rectilinear surface, see Fig. 1.

The position vector $\mathbf{y} = \chi(\mathbf{x})$ of the shell in the deformed placement $\overline{B} = \chi(B)$ can formally be represented by

$$\mathbf{y}(x,\xi) = \boldsymbol{y}(x) + \boldsymbol{\zeta}(x,\xi), \quad \boldsymbol{\zeta}(x,0) = \mathbf{0}, \tag{2}$$

where $\boldsymbol{y} = \chi(\boldsymbol{x})$ is the position vector of the deformed base surface $\overline{M} = \chi(M)$, which is a material surface during the deformation process, and $\boldsymbol{\zeta}$ is a deviation of $\mathrm{y} \in \overline{B}$ from the deformed base surface $\overline{M}$, see Fig. 1.

Let $P \subset B$ be an arbitrary part of the shell B with a boundary consisting of three separable parts: $\partial P = \Pi^+ \cup \Pi^- \cup \partial P^*$, where $\Pi^\pm \subset M^\pm$ and $\partial P^* \subset \partial B^*$. Then in the referential description the 3D global equilibrium conditions of P expressing the vanishing of the total force vector $\mathbf{F}(P)$ and the total torque vector $\mathbf{T}_\mathrm{o}(P)$ taken relative to an arbitrary point $\mathrm{o} \in \mathscr{E}$ of all forces acting on P are

$$\begin{aligned} \mathbf{F}(P) &= \int\int\int_P \mathbf{f}\,\mathrm{d}v + \int\int_{\partial P \setminus \partial B_f} \mathbf{t}_n\,\mathrm{d}a + \int\int_{\partial P \cap \partial B_f} \mathbf{t}^*\,\mathrm{d}a = \mathbf{0}, \\ \mathbf{T}_\mathrm{o}(P) &= \int\int\int_P \mathbf{y} \times \mathbf{f}\,\mathrm{d}v + \int\int_{\partial P \setminus \partial B_f} \mathbf{y} \times \mathbf{t}_n\,\mathrm{d}a + \int\int_{\partial P \cap \partial B_f} \mathbf{y} \times \mathbf{t}^*\,\mathrm{d}a = \mathbf{0}. \end{aligned} \tag{3}$$

In (3), ∂B_f is that part of ∂B on which the traction vector field $\mathbf{t}^*(\mathrm{x})$ is prescribed, $\mathbf{f}(\mathrm{x})$ is the volume force vector field, and $\mathbf{t}_n(\mathrm{x})$ is the contact force vector field. In shell theory it is usually assumed that the traction $\mathbf{t}^*$ is prescribed on both shell faces $M^\pm$ and on a part ∂B_f^* of the lateral boundary surface ∂B^*, Fig. 1.

If (1) and (2) are introduced into (3) one can perform an exact through-the-thickness integration with regard to the co-ordinate ξ. The global equilibrium conditions (3) can then be expressed through the resultant fields defined entirely on the reference base surface M. Such a resultant form of the conditions is appropriate for the 2D theory of shells. In case of a regular shell, such an exact reduction procedure with regard to a non-material weighted surface of mass was first suggested by Libai and Simmonds (1983), and with regard to a material base surface by Makowski and Stumpf (1990). In what follows we perform such an exact reduction of the equilibrium conditions (3) with regard to the material base surface in case of branching and self-intersecting shells.

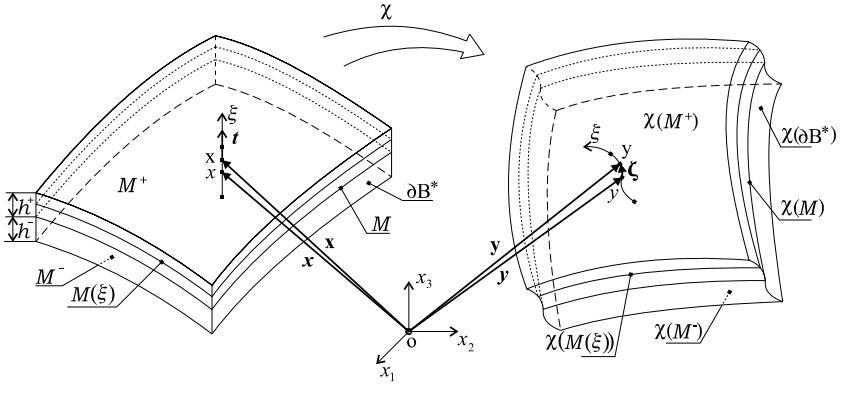

Fig. 1. Geometry of 3D shell-like body in the reference and deformed placements.

3. Branching shell

Let the reference shell B consist of three regular parts B_k, $k = 1,2,3$, rigidly connected together along the common junction, see Fig. 2(a). We assume that two regular parts B_1 and B_2 form together a regular shell $B_1 \cup B_2$ which lower face $M_1^- \cup M_2^-$ is a regular surface, Fig. 2(a). It is also assumed that the traction $\mathbf{t}^*$ can be prescribed, in general, on the upper M^+ and lower M^- shell faces as well as on the part ∂B_f^* of the lateral boundary surface ∂B^*. The reference base surface M of B can always be chosen to be located arbitrarily within the shell space and to consist of three regular surfaces M_k connected together along the common surface curve $\Gamma = \partial M_1 \cap \partial M_2 \cap \partial M_3$, as in Fig. 2(b). This means that each of B_k has to be treated as being extended into the junction region so that Γ should belong to the corresponding parts of each lateral boundary surface ∂B_k^* along the junction.

Cutting off an arbitrary part P of B containing the junction, let us discuss the exact reduction of its global equilibrium conditions (3) to the statically equivalent conditions written on the part of the reference base surface $\Pi \subset M$, where the shell parts P_k are represented by their corresponding images Π_k and Γ, see Fig. 2.

Extending each of the parts P_k into the junction region it is implicitly assumed that some fictitious tractions $\mathbf{t}^*$ are applied also on the shaded surface strips Π_{1d}^+, Π_{2d}^+, Π_{3d}^+, Π_{3d}^- at the junction region in Fig. 3. Then by through-the-thickness integration, the volume forces $\mathbf{f}(x)$ as well as the tractions $\mathbf{t}_n(x)$ and $\mathbf{t}^*(x)$ acting in each P_k are reduced to an equivalent system of forces and couples applied on the base surface $\Pi \subset M$. During the procedure there are two tubes P_{1d} and P_{2d} where the integration is performed twice: once when reducing the volume forces $\mathbf{f}(x)$ given in P_1, P_2 and the tractions $\mathbf{t}_n$ or $\mathbf{t}^*$ acting on ∂P_{1d} and ∂P_{2d} at x_i and x_e to their resultant forces and couples applied on Π_1, Π_2, respectively, and the second time when reducing $\mathbf{f}(x)$ given in P_3 and $\mathbf{t}_n$ or $\mathbf{t}^*$ acting on ∂P_{1d} and ∂P_{2d} at x_i and x_e to their equivalent forces and couples applied on Π_3. In order to compensate the surplus of forces and couples following from the fictitious tractions and the double integration, we have to subtract some forces and couples applied along Γ which are statically equivalent to those additionally introduced loads.

After performing integration with regard to ξ, the total force vector $\mathbf{F}_1(P_1)$ defined in $(3)_1$ of all spatial forces acting in P_1 and on ∂P_1 is given by

$$\mathbf{F}_1(\Pi_1) = \int\int_{\Pi_1} \boldsymbol{f}_1 \,\mathrm{d}a_1 + \int_{\partial\Pi_1 \setminus \partial M_f} \boldsymbol{n}_{1v} \,\mathrm{d}s + \int_{\partial\Pi_1 \cap \partial M_f} \boldsymbol{n}_1^* \,\mathrm{d}s - \int_\Gamma \boldsymbol{f}_{1\Gamma} \,\mathrm{d}s, \tag{4}$$

where

$$\begin{aligned} \boldsymbol{f}_1 &= \int_{-h_1^-}^{+h_1^+} \mathbf{f}_1 \mu_1 \,\mathrm{d}\xi_1 + \alpha_1^+ \mathbf{t}_1^{*+} - \alpha_1^- \mathbf{t}_1^{*-}, \\ \boldsymbol{n}_{1v} &= \int_{-h_1^-}^{+h_1^+} \alpha_1^* \mathbf{t}_{1n} \,\mathrm{d}\xi_1, \quad \boldsymbol{n}_1^* = \int_{-h_1^-}^{+h_1^+} \alpha_1^* \mathbf{t}_1^* \,\mathrm{d}\xi_1, \end{aligned} \tag{5}$$

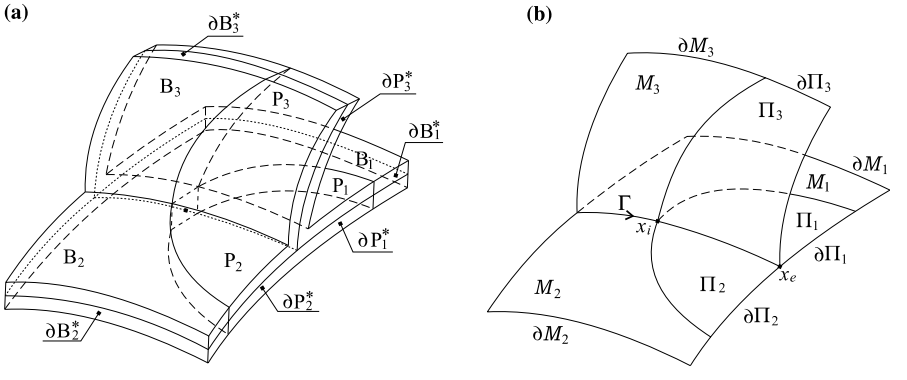

Fig. 2. The branching shell structure: (a) the 3D shell, and (b) the corresponding 2D base surface.

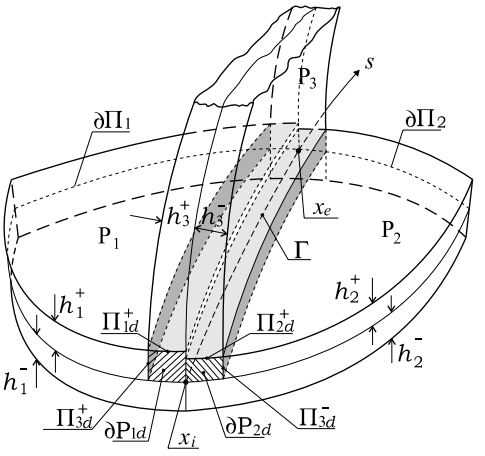

Fig. 3. Part of the branching shell: surface strips with fictitious forces and tubes of double integration.

with $\mathbf{t}_1^{*+}$ and $\mathbf{t}_1^{*-}$ denoting the tractions prescribed on Π_1^+ and Π_1^-, respectively, and ξ_1 the transverse co-ordinate of P_1.

The minus sign in front of $\alpha_1^-\mathbf{t}_1^{*-}$ in $(5)_1$ conventionally indicates that the traction $\mathbf{t}_1^{*-}$ acts on the surface M_1^- which outward orientation is opposite to the one of M_1^+, see (A.10).

The correcting force $\boldsymbol{f}_{1\Gamma}$ subtracted in (4) takes into account the fictitious traction $\mathbf{t}_1^{*+}$ applied on Π_{1d}^+ and included in definition $(5)_1$ of $\boldsymbol{f}_1$. The area element of Π_{1d}^+ is $\mathrm{d}a_1^+ = \alpha_1^+\,\mathrm{d}a_1$, according to $(A.12)_1$, where $\mathrm{d}a_1$ is the area element of Π_1. However, when extending P_1 into the branching region the extended part of Π_1 can always be chosen to coincide with the lateral boundary surface $\partial\Pi_3^*$. Therefore, $\mathrm{d}a_1$ may also be interpreted here as the area element $\mathrm{d}a_3^*$ of ∂P_3^* along the curve Γ. According to $(A.14)_1$, $\mathrm{d}a_3^* = \alpha_3^*\,\mathrm{d}\xi_3\,\mathrm{d}s$ and therefore

$$\int\int_{\Pi_{1d}^+}\mathbf{t}_1^{*+}\,\mathrm{d}a_1^+ = \int_\Gamma \boldsymbol{f}_{1\Gamma}\,\mathrm{d}s, \quad \boldsymbol{f}_{1\Gamma} = \int_0^{+h_3^+}\alpha_1^+\alpha_3^*\mathbf{t}_1^{*+}\,\mathrm{d}\xi_3. \tag{6}$$

In exactly the same way we can calculate the total force vector $\mathbf{F}_2(\Pi_2)$ of all spatial forces acting on P_2. The result is expressed through the fields defined on Π_2 and $\partial\Pi_2$ in complete analogy to those given in (5) and (6):

$$\mathbf{F}_2(\Pi_2) = \int\int_{\Pi_2}\boldsymbol{f}_2\,\mathrm{d}a_2 + \int_{\partial\Pi_2\setminus\partial M_f}\boldsymbol{n}_{2\nu}\,\mathrm{d}s + \int_{\partial\Pi_2\cap\partial M_f}\boldsymbol{n}_2^*\,\mathrm{d}s - \int_\Gamma \boldsymbol{f}_{2\Gamma}\,\mathrm{d}s, \tag{7}$$

where

$$\begin{aligned}
\boldsymbol{f}_2 &= \int_{-h_2^-}^{+h_2^+}\mathbf{f}_2\mu_2\,\mathrm{d}\xi_2 + \alpha_2^+\mathbf{t}_2^{*+} - \alpha_2^-\mathbf{t}_2^{*-},\\
\boldsymbol{n}_{2\nu} &= \int_{-h_2^-}^{+h_2^+}\alpha_2^*\mathbf{t}_{2n}\,\mathrm{d}\xi_2, \quad \boldsymbol{n}_2^* = \int_{-h_2^-}^{+h_2^+}\alpha_2^*\mathbf{t}_2^*\,\mathrm{d}\xi_2,\\
\boldsymbol{f}_{2\Gamma} &= \int_{-h_3^-}^{0}\alpha_2^+\alpha_3^*\mathbf{t}_2^{*+}\,\mathrm{d}\xi_3.
\end{aligned} \tag{8}$$

The total force vector $\mathbf{F}_3(\Pi_3)$ is calculated by direct integration in $(3)_1$ with regard to ξ_3 leading to

$$\mathbf{F}_3(\Pi_3) = \int\int_{\Pi_3}\boldsymbol{f}_3\,\mathrm{d}a_3 + \int_{\partial\Pi_3\setminus\partial M_f}\boldsymbol{n}_{3\nu}\,\mathrm{d}s + \int_{\partial\Pi_3\cap\partial M_f}\boldsymbol{n}_3^*\,\mathrm{d}s - \int_\Gamma \boldsymbol{f}_{3\Gamma}\,\mathrm{d}s - (\boldsymbol{n}_{3e} - \boldsymbol{n}_{3i}), \tag{9}$$

where

$$\boldsymbol{f}_3 = \int_{-h_3^-}^{+h_3^+} \mathbf{f}_3 \mu_3 \,\mathrm{d}\xi_3 + \alpha_3^+ \mathbf{t}_3^{*+} - \alpha_3^- \mathbf{t}_3^{*-},$$
$$\boldsymbol{n}_{3v} = \int_{-h_3^-}^{+h_3^+} \alpha_3^* \mathbf{t}_{3n} \,\mathrm{d}\xi_3, \quad \boldsymbol{n}_3^* = \int_{-h_3^-}^{+h_3^+} \alpha_3^* \mathbf{t}_3^* \,\mathrm{d}\xi_3. \tag{10}$$

The correcting force $\boldsymbol{f}_{3\Gamma}$ in (9) should again take into account fictitious tractions $\mathbf{t}_3^{*\pm}$ applied on $\Pi_{3d}^{\pm}$ and included in definition $(10)_1$ of $\boldsymbol{f}_3$. The area elements of $\Pi_{3d}^{\pm}$ are $\mathrm{d}a_3^{\pm} = \alpha_3^{\pm}\,\mathrm{d}a_3$, according to $(A.12)_1$. When transforming the elementary traction $\mathbf{t}_3^{*+}\,\mathrm{d}a_3^+$ the area element $\mathrm{d}a_3$ may be changed into $\mathrm{d}a_1^* = \alpha_1^*\,\mathrm{d}\xi_1\,\mathrm{d}s$ of ∂P_1^* along Γ. Similarly, when transforming $-\mathbf{t}_3^{*-}\,\mathrm{d}a_3^-$ the area element $\mathrm{d}a_3$ may be changed into $\mathrm{d}a_2^* = \alpha_2^*\,\mathrm{d}\xi_2\,\mathrm{d}s$ of ∂P_2^* along Γ.

The first term in definition $(10)_1$ of $\boldsymbol{f}_3$ also includes the volume force field $\mathbf{f}_3$ applied within the tubes P_{1d} and P_{2d}. These volume forces have already been taken into account in definitions $(5)_1$ of $\boldsymbol{f}_1$ and $(8)_1$ of $\boldsymbol{f}_2$, respectively. In order to correct the result of the double integration, we have to subtract an equivalent force resultant field by including it into definition of $\boldsymbol{f}_{3\Gamma}$ acting along Γ. Since in P_{1d}, according to $(A.3)_1$, the elementary volume force is $\mathbf{f}_3\,\mathrm{d}v_3 = \mathbf{f}_3\mu_3\,\mathrm{d}\xi_3\,\mathrm{d}a_3$ and $\mathrm{d}a_3$ can be changed into $\mathrm{d}a_1^* = \alpha_1^*\,\mathrm{d}\xi_1\,\mathrm{d}s$, we can integrate $\mathbf{f}_3\,\mathrm{d}v_3$ over the surface ∂P_{1d}. Similarly, since in P_{2d} the elementary volume force is again $\mathbf{f}_3\,\mathrm{d}v_3 = \mathbf{f}_3\mu_3\,\mathrm{d}\xi_3\,\mathrm{d}a_3$ but now $\mathrm{d}a_3$ can be changed into $\mathrm{d}a_2^* = \alpha_2^*\,\mathrm{d}\xi_2\,\mathrm{d}s$, we can integrate $\mathbf{f}_3\,\mathrm{d}v_3$ over the surface ∂P_{2d}.

As a result of all those transformations we obtain

$$\int\int_{\Pi_{3d}^+} \mathbf{t}_3^{*+}\,\mathrm{d}a_3^+ - \int\int_{\Pi_{3d}^-} \mathbf{t}_3^{*-}\,\mathrm{d}a_3^- + \int\int\int_{P_{1d}} \mathbf{f}_3\,\mathrm{d}v_3 + \int\int\int_{P_{2d}} \mathbf{f}_3\,\mathrm{d}v_3 = \int_\Gamma \boldsymbol{f}_{3\Gamma}\,\mathrm{d}s,$$
$$\boldsymbol{f}_{3\Gamma} = \int_0^{+h_1^+} \alpha_3^+\alpha_1^*\mathbf{t}_3^{*+}\,\mathrm{d}\xi_1 - \int_0^{+h_2^+} \alpha_3^-\alpha_2^*\mathbf{t}_3^{*-}\,\mathrm{d}\xi_2 \tag{11}$$
$$+ \int_0^{+h_1^+} \left(\int_0^{+h_3^+} \mathbf{f}_3\mu_3\,\mathrm{d}\xi_3\right)\alpha_1^*\,\mathrm{d}\xi_1 + \int_0^{+h_2^+} \left(\int_{-h_3^-}^{0} \mathbf{f}_3\mu_3\,\mathrm{d}\xi_3\right)\alpha_2^*\,\mathrm{d}\xi_2.$$

When reducing the elementary tractions $\mathbf{t}_{3n}\,\mathrm{d}a_3^*$ or $\mathbf{t}_3^*\,\mathrm{d}a_3^*$ acting on $\partial P_3^* \setminus \partial B_f^*$ or $\partial P_3^* \cap \partial B_f^*$ to the resultant boundary forces $\boldsymbol{n}_{3v}$ or $\boldsymbol{n}_3^*$ acting on $\partial\Pi_3\backslash\partial M_f$ or $\partial\Pi_3 \cap \partial M_f$, respectively, we note that the tractions acting on the boundaries ∂P_{1d} and ∂P_{2d} at x_i have already been taken into account in the expressions (4) and (7). In order to correct the result of the double integration in (9), we have to subtract in (9) some statically equivalent concentrated forces $\boldsymbol{n}_{3i}$ or $\boldsymbol{n}_{3i}^*$ acting at the initial point x_i of Γ and defined by

$$\boldsymbol{n}_{3i} = \int\int_{(\partial P_{1d}\cup\partial P_{2d})\backslash\partial B_f^*} \mathbf{t}_{3n}\,\mathrm{d}a_3^*, \quad \boldsymbol{n}_{3i}^* = \int\int_{(\partial P_{1d}\cup\partial P_{2d})\cap\partial B_f^*} \mathbf{t}_3^*\,\mathrm{d}a_3^*. \tag{12}$$

In exactly the same way we can define the statically equivalent concentrated forces $\boldsymbol{n}_{3e}$ or $\boldsymbol{n}_{3e}^*$ acting at the end point x_e of Γ. The second minus sign in front of $\boldsymbol{n}_i$ in (9) conventionally indicates that the boundaries ∂P_{1d} and ∂P_{2d} at x_i have opposite orientations than the orientation of Γ. Similar boundaries at x_e have the same orientations as the one of Γ.

Summing up the results for $\mathbf{F}_1$, $\mathbf{F}_2$, $\mathbf{F}_3$ we can write

$$\mathbf{F}(\Pi) = \int\int_{\Pi\setminus\Gamma} \boldsymbol{f}\;\mathrm{d}a + \int_{\partial\Pi\setminus\partial M_f} \boldsymbol{n}_v\,\mathrm{d}s + \int_{\partial M_f} \boldsymbol{n}^*\,\mathrm{d}s - \int_\Gamma \boldsymbol{f}_\Gamma\,\mathrm{d}s - (\boldsymbol{n}_e - \boldsymbol{n}_i). \tag{13}$$

In (13) the resultant surface forces $\boldsymbol{f}$, the surface stress resultants $\boldsymbol{n}_v$, the resultant boundary forces $\boldsymbol{n}^*$, and the compensating curvilinear force resultants $\boldsymbol{f}_\Gamma$ follow from all three parts of P, while the concentrated forces $\boldsymbol{n}_i$, $\boldsymbol{n}_e$ follow only from integration over ∂P_{1d} and ∂P_{2d} taken into account in $\mathbf{F}_3(\Pi_3)$.

The total torque vector $\mathbf{T}_o(\Pi)$ relative to $o \in \mathscr{E}$ of all spatial forces acting on P can again be calculated by direct integration in $(3)_2$ with regard to ξ. The procedure is exactly the same as in (4)–(13), only when calculating the surface couples one has to introduce the following exact representations (2) for the 3D position vector in the deformed placement relative to the deformed base surface $\chi(M)$:

$$\mathbf{y} = \boldsymbol{y} + \boldsymbol{\zeta}, \quad \mathbf{y}^+ = \boldsymbol{y} + \boldsymbol{\zeta}^+, \quad \mathbf{y}^- = \boldsymbol{y} + \boldsymbol{\zeta}^-. \tag{14}$$

In the tubes P_{1d} and P_{2d} the compensating couples should be reduced relative to points of the deformed singular curve $\chi(\Gamma)$, and the position vectors in the deformed placement should be taken in the following exact form:

$$\mathbf{y} = \boldsymbol{y}_\Gamma + \boldsymbol{\zeta}_\Gamma, \quad \mathbf{y}^+ = \boldsymbol{y}_\Gamma + \boldsymbol{\zeta}_\Gamma^+, \quad \mathbf{y}^- = \boldsymbol{y}_\Gamma + \boldsymbol{\zeta}_\Gamma^-. \tag{15}$$

After performing integration with regard to ξ_1, the total torque vector $\mathbf{T}_{o1}(\Pi_1)$ defined in $(3)_2$ of all spatial forces acting in P_1 and on ∂P_1 is given by

$$\begin{aligned}\mathbf{T}_{o1}(\Pi_1) = &\int\int_{\Pi_1} (\boldsymbol{c}_1 + \boldsymbol{y}_1 \times \boldsymbol{f}_1)\,\mathrm{d}a_1 + \int_{\partial\Pi_1\setminus\partial M_f} (\boldsymbol{m}_{1\nu} + \boldsymbol{y}_1 \times \boldsymbol{n}_{1\nu})\,\mathrm{d}s + \int_{\partial\Pi_1\cap\partial M_f} (\boldsymbol{m}_1^* + \boldsymbol{y}_1 \times \boldsymbol{n}_1^*)\,\mathrm{d}s \\ &- \int_\Gamma (\boldsymbol{c}_{1\Gamma} + \boldsymbol{y}_\Gamma \times \boldsymbol{f}_{1\Gamma})\,\mathrm{d}s,\end{aligned} \tag{16}$$

where now

$$\begin{aligned}\boldsymbol{c}_1 &= \int_{-h_1^-}^{+h_1^+} \boldsymbol{\zeta}_1 \times \mathbf{f}_1 \mu_1\,\mathrm{d}\xi_1 + \alpha_1^+ \boldsymbol{\zeta}_1^+ \times \mathbf{t}_1^{*+} - \alpha_1^- \boldsymbol{\zeta}_1^- \times \mathbf{t}_1^{*-}, \\ \boldsymbol{m}_{1\nu} &= \int_{-h_1^-}^{+h_1^+} \alpha_1^* \boldsymbol{\zeta}_1 \times \mathbf{t}_{1n}\,\mathrm{d}\xi_1, \quad \boldsymbol{m}_1^* = \int_{-h_1^-}^{+h_1^+} \alpha_1^* \boldsymbol{\zeta}_1 \times \mathbf{t}_1^*\,\mathrm{d}\xi_1, \\ \boldsymbol{c}_{1\Gamma} &= \int_0^{+h_3^+} \alpha_1^+ \alpha_3^* \boldsymbol{\zeta}_{1\Gamma}^+ \times \mathbf{t}_1^{*+}\,\mathrm{d}\xi_3.\end{aligned} \tag{17}$$

In exactly the same way we can calculate the total torque vector $\mathbf{T}_{o2}(\Pi_2)$ of all spatial forces acting in P_2 and on ∂P_2, and the result is

$$\begin{aligned}\mathbf{T}_{o2}(\Pi_2) = &\int\int_{\Pi_2} (\boldsymbol{c}_2 + \boldsymbol{y}_2 \times \boldsymbol{f}_2)\,\mathrm{d}a_2 + \int_{\partial\Pi_2\setminus\partial M_f} (\boldsymbol{m}_{2\nu} + \boldsymbol{y}_2 \times \boldsymbol{n}_{2\nu})\,\mathrm{d}s + \int_{\partial\Pi_2\cap\partial M_f} (\boldsymbol{m}_2^* + \boldsymbol{y}_2 \times \boldsymbol{n}_2^*)\,\mathrm{d}s \\ &- \int_\Gamma (\boldsymbol{c}_{2\Gamma} + \boldsymbol{y}_\Gamma \times \boldsymbol{f}_{2\Gamma})\,\mathrm{d}s,\end{aligned} \tag{18}$$

where $\boldsymbol{c}_2$, $\boldsymbol{m}_{2\nu}$, $\boldsymbol{m}_2^*$, $\boldsymbol{c}_{2\Gamma}$ are defined in complete analogy to the fields (17).

Finally, the total torque vector $\mathbf{T}_{o3}(\Pi_3)$ of all spatial forces acting in P_3 and on ∂P_3 reads

$$\begin{aligned}\mathbf{T}_{o3}(\Pi_3) = &\int\int_{\Pi_3} (\boldsymbol{c}_3 + \boldsymbol{y}_3 \times \boldsymbol{f}_3)\,\mathrm{d}a_3 + \int_{\partial\Pi_3\setminus\partial M_f} (\boldsymbol{m}_{3\nu} + \boldsymbol{y}_3 \times \boldsymbol{n}_{3\nu})\,\mathrm{d}s + \int_{\partial\Pi_3\cap\partial M_f} (\boldsymbol{m}_3^* + \boldsymbol{y}_3 \times \boldsymbol{n}_3^*)\,\mathrm{d}s \\ &- \int_\Gamma (\boldsymbol{c}_{3\Gamma} + \boldsymbol{y}_\Gamma \times \boldsymbol{f}_{3\Gamma})\,\mathrm{d}s - \{(\boldsymbol{m}_{3e} + \boldsymbol{y}_{\Gamma e} \times \boldsymbol{n}_{3e}) - (\boldsymbol{m}_{3i} + \boldsymbol{y}_{\Gamma i} \times \boldsymbol{n}_{3i})\},\end{aligned} \tag{19}$$

where all 2D and 1D fields are defined analogously to (17), and the compensating couples are defined in analogy to $(11)_2$ by

$$\begin{aligned}\boldsymbol{c}_{3\Gamma} = &\int_0^{+h_1^+} \alpha_3^+ \alpha_1^* \boldsymbol{\zeta}_{3\Gamma}^+ \times \mathbf{t}_3^{*+}\,\mathrm{d}\xi_1 - \int_0^{+h_2^+} \alpha_3^- \alpha_2^* \boldsymbol{\zeta}_{3\Gamma}^+ \times \mathbf{t}_3^{*-}\,\mathrm{d}\xi_2 \\ &+ \int_0^{+h_1^+} \left(\int_0^{+h_3^+} \boldsymbol{\zeta}_\Gamma \times \mathbf{f}_3 \mu_3\,\mathrm{d}\xi_3\right) \alpha_1^*\,\mathrm{d}\xi_1 + \int_0^{+h_2^+} \left(\int_{-h_3^-}^0 \boldsymbol{\zeta}_\Gamma \times \mathbf{f}_3 \mu_3\,\mathrm{d}\xi_3\right) \alpha_2^*\,\mathrm{d}\xi_2, \\ \boldsymbol{m}_{3i} = &\int\int_{(\partial P_{1d}\cup\partial P_{2d})\setminus\partial B_f^*} \boldsymbol{\zeta}_\Gamma \times \mathbf{t}_{3n}\,\mathrm{d}a_3^*,\end{aligned} \tag{20}$$

with similar apparent definitions for $\boldsymbol{m}_{3i}^*$, $\boldsymbol{m}_{3e}$, and $\boldsymbol{m}_{3e}^*$.

Summing up the results for $\mathbf{T}_{o1}(\Pi_1)$, $\mathbf{T}_{o2}(\Pi_2)$, and $\mathbf{T}_{o3}(\Pi_3)$ and performing some transformations we obtain the total torque vector $\mathbf{T}_o(\Pi)$ of the branched shell expressed only by the fields defined on an arbitrary part Π of the base surface

$$\mathbf{T}_o(\Pi) = \int\int_{\Pi\setminus\Gamma} (\boldsymbol{c} + \boldsymbol{y}\times\boldsymbol{f})\,\mathrm{d}a + \int_{\partial\Pi\setminus\partial M_f} (\boldsymbol{m}_\nu + \boldsymbol{y}\times\boldsymbol{n}_\nu)\,\mathrm{d}s + \int_{\partial M_f} (\boldsymbol{m}^* + \boldsymbol{y}\times\boldsymbol{n}^*)\,\mathrm{d}s - \int_\Gamma (\boldsymbol{c}_\Gamma + \boldsymbol{y}_\Gamma\times\boldsymbol{f}_\Gamma)\,\mathrm{d}s - \{(\boldsymbol{m}_e + \boldsymbol{y}_{\Gamma e}\times\boldsymbol{n}_e) - (\boldsymbol{m}_i + \boldsymbol{y}_{\Gamma i}\times\boldsymbol{n}_i)\}. \tag{21}$$

Again, in (21) the resultant surface couples $\boldsymbol{c}$, the resultant stress couples $\boldsymbol{m}_\nu$, the resultant boundary couples $\boldsymbol{m}^*$, and the compensating curvilinear couple resultants $\boldsymbol{c}_\Gamma$ follow from all three parts of P, while the concentrated couples $\boldsymbol{m}_i$, $\boldsymbol{m}_e$ follow only from integration over ∂P_{1d} and ∂P_{2d} taken into account in $\mathbf{T}_{o3}(\Pi_3)$.

The relations (13) and (21) are exact 2D static equivalents of $\mathbf{F}(P)$ and $\mathbf{T}_o(P)$ appearing in the 3D global equilibrium conditions (3) for an arbitrary part P of the branching shell B treated as a 3D solid body.

4. Transformations

The global equilibrium conditions (3), with the total force and torque vectors expressed through the surface fields by (13) and (21), should now be appropriately transformed.

Let the surface point $x \in M$ be a regular point of ∂M. Then by the surface Cauchy theorem there exist the surface stress resultant tensor $\boldsymbol{N}(x) \in E \otimes T_xM$ and the surface stress couple tensor $\boldsymbol{M}(x) \in E \otimes T_xM$, both of the 1st Piola–Kirchhoff type, such that

$$\boldsymbol{n}_\nu = \boldsymbol{N}\boldsymbol{\nu}, \quad \boldsymbol{m}_\nu = \boldsymbol{M}\boldsymbol{\nu}, \tag{22}$$

where T_xM is the 2D vector space tangent to M at $x \in M$, and $\boldsymbol{\nu} \in T_xM$ is the unit vector externally normal to ∂M.

For any tensor field $\boldsymbol{S} \in F \otimes T_xM$, where F denotes a vector space, the generalized divergence theorem at the piecewise smooth surface M, consisting of n regular surface elements M_k joined along the common junction represented by the stationary singular curve Γ, has the form (Chróścielewski et al., 2004, see formula 1.4.39)

$$\int\int_{M\setminus\Gamma} \mathrm{Div}\boldsymbol{S}\,\mathrm{d}a = \int_{\partial M} \boldsymbol{S}\boldsymbol{\nu}\,\mathrm{d}s + \int_\Gamma [\boldsymbol{S}\boldsymbol{\nu}]\,\mathrm{d}s. \tag{23}$$

Here Div is the surface divergence operator on M defined intrinsically by Gurtin and Murdoch (1975), and the jump at each regular point of Γ is defined by

$$[\boldsymbol{S}\boldsymbol{\nu}] = \sum_{k=1}^{n} \boldsymbol{S}_k\boldsymbol{\nu}_k, \tag{24}$$

where $\boldsymbol{S}_k$ is the one-sided finite limit of $\boldsymbol{S}$ when the respective boundary ∂M_k coinciding with Γ is approached, and $\boldsymbol{\nu}_k \in T_xM_k$ is the unit vector externally normal to ∂M_k.

In particular, if we apply (23) to some terms present in (13) and (21) we obtain

$$\begin{aligned}
\int_{\partial\Pi} \boldsymbol{N}\boldsymbol{\nu}\,\mathrm{d}s &= \int\int_{\Pi\setminus\Gamma} \mathrm{Div}\boldsymbol{N}\,\mathrm{d}a - \int_\Gamma [\boldsymbol{N}\boldsymbol{\nu}]\,\mathrm{d}s,\\
\int_{\partial\Pi} \boldsymbol{M}\boldsymbol{\nu}\,\mathrm{d}s &= \int\int_{\Pi\setminus\Gamma} \mathrm{Div}\boldsymbol{M}\,\mathrm{d}a - \int_\Gamma [\boldsymbol{M}\boldsymbol{\nu}]\,\mathrm{d}s,\\
\int_{\partial\Pi} \boldsymbol{y}\times\boldsymbol{N}\boldsymbol{\nu}\,\mathrm{d}s &= \int\int_{\Pi\setminus\Gamma} \{ax(\boldsymbol{N}\boldsymbol{F}^{\mathrm{T}} - \boldsymbol{F}\boldsymbol{N}^{\mathrm{T}}) + \boldsymbol{y}\times(\mathrm{Div}\boldsymbol{N})\}\,\mathrm{d}a - \int_\Gamma [\boldsymbol{y}\times\boldsymbol{N}\boldsymbol{\nu}]\,\mathrm{d}s,
\end{aligned} \tag{25}$$

where $ax(\cdot)$ means the axial vector of the skew tensor $(\cdot)$, $\boldsymbol{F} = \nabla\boldsymbol{y} \in E \otimes T_xM$ is the shell deformation gradient with ∇ the surface gradient operator on M, and for the branching shell discussed here

$$[\boldsymbol{N}\boldsymbol{v}] = \sum_{k=1}^{3} \boldsymbol{N}_k \boldsymbol{v}_k, \quad [\boldsymbol{M}\boldsymbol{v}] = \sum_{k=1}^{3} \boldsymbol{M}_k \boldsymbol{v}_k,$$
$$[\boldsymbol{y} \times \boldsymbol{N}\boldsymbol{v}] = \sum_{k=1}^{3} \boldsymbol{y}_k \times \boldsymbol{N}_k \boldsymbol{v}_k. \tag{26}$$

Note that the second terms of (13) and (21) are integrated along $\partial\Pi\backslash\partial M_f$, while in the left-hand sides of (25) there are integrations over the full boundary $\partial\Pi$. In order to apply (25), one has to insert into (13) and (21) $\pm$ integrals over $\partial\Pi \cap \partial M_f$ with the same integrands as in the second terms of (13) and (21), respectively. Then these additional integrals with $+$ sign complete the second terms of (13) and (21) into the integrals over the full $\partial\Pi$, while the integrals with $-$ sign can be combined with the respective third integrals of (13) and (21). This allows one to use the generalized divergence theorems (25) to all terms integrated over $\partial\Pi$ in (13) and (21).

Finally, note that the last two terms of (13) and (21) are just some concentrated loads applied at the both ends of the singular curve Γ. Thus, we can equivalently represent them by the following curvilinear integrals over some distributed loads along Γ:

$$\boldsymbol{n}_e - \boldsymbol{n}_i = \int_\Gamma \boldsymbol{n}' \,\mathrm{d}s,$$
$$(\boldsymbol{m}_e + \boldsymbol{y}_{\Gamma e} \times \boldsymbol{n}_e) - (\boldsymbol{m}_i + \boldsymbol{y}_{\Gamma i} \times \boldsymbol{n}_i) = \int_\Gamma (\boldsymbol{m}' + \boldsymbol{y}'_\Gamma \times \boldsymbol{n} + \boldsymbol{y}_\Gamma \times \boldsymbol{n}') \,\mathrm{d}s. \tag{27}$$

As a result of all transformations suggested above the global equilibrium conditions (13) and (21) for the branching shell take the forms

$$\mathbf{F}(\Pi) = \int\int_{\Pi\backslash\Gamma} (\mathrm{Div}\boldsymbol{N} + \boldsymbol{f}) \,\mathrm{d}a + \int_{\partial M_f} (\boldsymbol{n}^* - \boldsymbol{N}\boldsymbol{v}) \,\mathrm{d}s$$
$$- \int_{\Pi\cap\Gamma} (\boldsymbol{n}' + [\boldsymbol{N}\boldsymbol{v}] + \boldsymbol{f}_\Gamma) \,\mathrm{d}s = \boldsymbol{0}, \tag{28}$$

$$\mathbf{T}_{\mathrm{o}}(\Pi) = \int\int_{\Pi\backslash\Gamma} \{\mathrm{Div}\boldsymbol{M} + ax(\boldsymbol{N}\boldsymbol{F}^{\mathrm{T}} - \boldsymbol{F}\boldsymbol{N}^{\mathrm{T}}) + \boldsymbol{c} + \boldsymbol{y} \times (\mathrm{Div}\boldsymbol{N} + \boldsymbol{f})\} \,\mathrm{d}a$$
$$+ \int_{\partial M_f} \{(\boldsymbol{m}^* - \boldsymbol{M}\boldsymbol{v}) + \boldsymbol{y} \times (\boldsymbol{n}^* - \boldsymbol{N}\boldsymbol{v})\} \,\mathrm{d}s$$
$$- \int_\Gamma \{\boldsymbol{m}' + \boldsymbol{y}'_\Gamma \times \boldsymbol{n} + [\boldsymbol{M}\boldsymbol{v}] + \boldsymbol{c}_\Gamma + \boldsymbol{y}_\Gamma \times (\boldsymbol{n}' + [\boldsymbol{N}\boldsymbol{v}] + \boldsymbol{f}_\Gamma)\} \,\mathrm{d}s = \boldsymbol{0}. \tag{29}$$

The relations (28) and (29) are again the exact static equivalents of the 3D global equilibrium conditions (3). However, now $\mathbf{F}(\Pi)$ and $\mathbf{T}_{\mathrm{o}}(\Pi)$ are expressed through the surface and curvilinear resultant fields referred to an arbitrary part Π of the reference base surface M, which corresponds to an arbitrary part P of the reference shell B treated as a 3D solid body.

5. Local dynamic conditions

Vanishing of the total force in (28) and the total torque in (29) requires that the following local dynamic conditions be satisfied:

the equilibrium equations

$$\mathrm{Div}\boldsymbol{N} + \boldsymbol{f} = \boldsymbol{0}, \quad \mathrm{Div}\boldsymbol{M} + ax(\boldsymbol{N}\boldsymbol{F}^{\mathrm{T}} - \boldsymbol{F}\boldsymbol{N}^{\mathrm{T}}) + \boldsymbol{c} = \boldsymbol{0} \tag{30}$$

at each regular point $x \in M\backslash\Gamma$,

the dynamic boundary conditions

$$\boldsymbol{n}^* - \boldsymbol{N}\boldsymbol{v} = \boldsymbol{0}, \quad \boldsymbol{m}^* - \boldsymbol{M}\boldsymbol{v} = \boldsymbol{0} \tag{31}$$

at each regular point $x \in \partial M_f$, and

the dynamic continuity conditions

$$\boldsymbol{n}' + [\boldsymbol{N}\boldsymbol{v}] + \boldsymbol{f}_\Gamma = \boldsymbol{0}, \quad \boldsymbol{m}' + \boldsymbol{y}'_\Gamma \times \boldsymbol{n} + [\boldsymbol{M}\boldsymbol{v}] + \boldsymbol{c}_\Gamma = \boldsymbol{0} \tag{32}$$

at each regular point $x \in \Gamma$.

Additionally, the dynamic boundary conditions

$$\begin{aligned} &\boldsymbol{n}_i^* - \boldsymbol{n}_i = \boldsymbol{0}, \quad \boldsymbol{m}_i^* - \boldsymbol{m}_i = \boldsymbol{0} \quad \text{at} \quad x_i \in \Gamma \cap \partial M_f, \\ &\boldsymbol{n}_e^* - \boldsymbol{n}_e = \boldsymbol{0}, \quad \boldsymbol{m}_e^* - \boldsymbol{m}_e = \boldsymbol{0} \quad \text{at} \quad x_e \in \Gamma \cap \partial M_f, \end{aligned} \tag{33}$$

have implicitly been used in (27) to account for the statically equivalent loads $\boldsymbol{n}$ and $\boldsymbol{m}$ applied along Γ.

The local relations (30) and (31) are equivalent, as one would expect, to the exact, resultant equilibrium equations and dynamic boundary conditions of the general non-linear theory of regular shells given, for example, in Libai and Simmonds (1983, 1998), Simmonds (1984), Makowski and Stumpf (1990), Pietraszkiewicz (2001a), Chróścielewski et al. (2004) and Eremeyev and Pietraszkiewicz (2004).

The dynamic continuity conditions (32) and (33) are the new exact, resultant relations that have to be satisfied along the singular curve Γ modelling the shell branching. They generalize two different forms of jump conditions proposed by Makowski et al. (1999) and Pietraszkiewicz (2001b) for two alternative formulations of the Kirchhoff–Love type non-linear theory of thin irregular shells. The conditions (32) complete by the correcting terms $\boldsymbol{n}$, $\boldsymbol{m}$, $\boldsymbol{f}_\Gamma$ and $\boldsymbol{c}_\Gamma$ the dynamic continuity conditions discussed in Makowski and Stumpf (1994), Chróścielewski et al. (1997) and Pietraszkiewicz (2001a), and make exact somewhat similar relations along Γ derived by Chróścielewski et al. (2004) using an alternative approximate procedure.

The conditions (32) are the ordinary differential equations along Γ which differ from the equilibrium equations of rods by the jump terms describing interactions between regular shell parts along the junction.

6. Self-intersecting shell

Let the shell B consist of two regular shell elements intersecting each other, see Fig. 4(a). Alternatively, we can think of the self-intersecting shell as consisting of four regular branches B_k, $k = 1, 2, 3, 4$, rigidly connected along the common junction. The reference base surface M of B consists now of four regular surfaces M_k rigidly connected along the common singular curve $\Gamma = \partial M_1 \cap \partial M_2 \cap \partial M_3 \cap \partial M_4$, as in Fig. 4(b).

Cutting off an arbitrary part P of B containing the junction, we can discuss again the exact reduction of the global equilibrium conditions (3) of P in the way discussed in Sections 3–5, only now we have additionally to take into account the existence of the fourth branch P_4, see Fig. 5. Thus, additionally to the shaded surface strips Π_{1d}^+, Π_{2d}^+, Π_{3d}^-, Π_{3d}^+ in Fig. 3, there appear other shaded surface strips Π_{1d}^-, Π_{2d}^-, Π_{4d}^-, Π_{4d}^+ in Fig. 5 on which some fictitious tractions are applied. There are now two enlarged tubes P_{1d} and P_{2d} with enlarged ends ∂P_{1d} and ∂P_{2d} at x_i and x_e, where the integration is performed twice. Therefore, in order to compensate the surplus of forces and couples following from the fictitious tractions and the double integration, we have to subtract again some forces and couples along Γ which are statically equivalent to the additionally introduced loads.

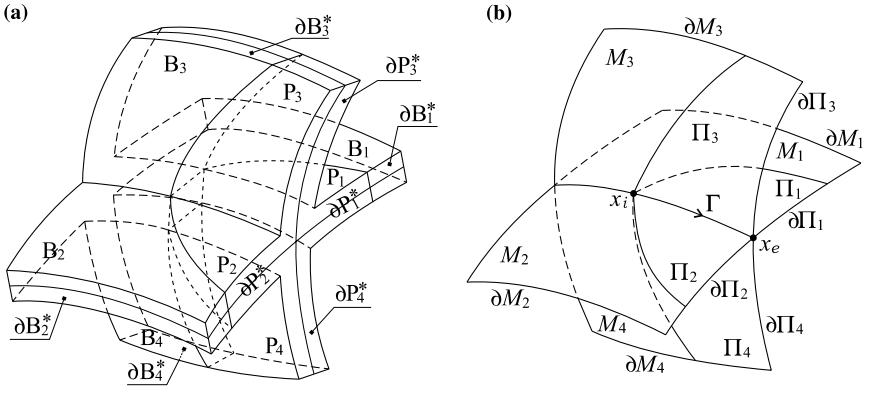

Fig. 4. The self-intersecting shell structure: (a) the 3D shell, and (b) the corresponding 2D base surface.

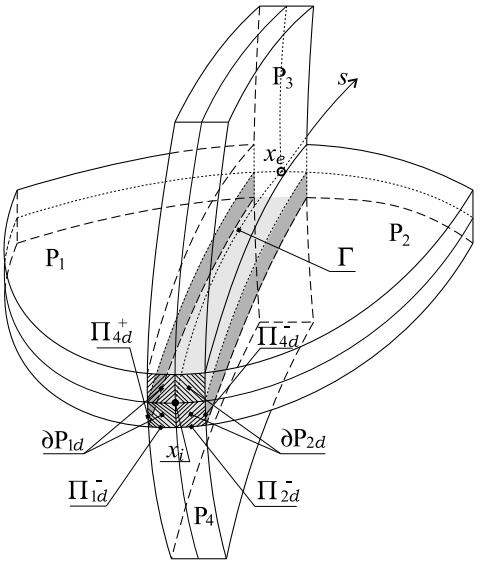

Fig. 5. Part of the self-intersecting shell: additional surface strips with fictitious forces and regions of double integration.

The expressions of the total forces $\mathbf{F}_k(\Pi_k)$ and the total torques $\mathbf{T}_{ok}(\Pi_k)$, $k = 1, 2, 3$, for the self-intersecting shell become here formally exactly the same as those given in Section 3 for the branching shell. However, some definitions of the correcting forces and couples applied along Γ have to be refined here as a result of existence of the additional part P_4.

Note that the area element of Π^-_{1d} is $\mathrm{d}a^-_1 = \alpha^-_1\,\mathrm{d}a_1$, where $\mathrm{d}a_1$ can now be changed into $\mathrm{d}a^*_4 = \alpha^*_4\,\mathrm{d}\xi_4\,\mathrm{d}s$. Therefore, the relations (6) for $\boldsymbol{f}_{1\Gamma}$ and $(17)_3$ for $\boldsymbol{c}_{1\Gamma}$ have to be refined now into

$$\begin{aligned}
&\int\int_{\Pi^+_{1d}} \mathbf{t}^{*+}_1\,\mathrm{d}a^+_1 - \int\int_{\Pi^-_{1d}} \mathbf{t}^{*-}_1\,\mathrm{d}a^-_1 = \int_\Gamma \boldsymbol{f}_{1\Gamma}\,\mathrm{d}s,\\
&\boldsymbol{f}_{1\Gamma} = \int_0^{+h^+_3} \alpha^+_1\alpha^*_3\mathbf{t}^{*+}_1\,\mathrm{d}\xi_3 - \int_0^{+h^+_4} \alpha^-_1\alpha^*_4\mathbf{t}^{*-}_1\,\mathrm{d}\xi_4,\\
&\boldsymbol{c}_{1\Gamma} = \int_0^{+h^+_3} \alpha^+_1\alpha^*_3\boldsymbol{\zeta}^+_{1\Gamma}\times\mathbf{t}^{*+}_1\,\mathrm{d}\xi_3 - \int_0^{+h^+_4} \alpha^-_1\alpha^*_4\boldsymbol{\zeta}^-_{1\Gamma}\times\mathbf{t}^{*-}_1\,\mathrm{d}\xi_4.
\end{aligned} \tag{34}$$

Similarly, the area element of Π^-_{2d} is $\mathrm{d}a^-_2 = \alpha^-_2\,\mathrm{d}a_2$, where $\mathrm{d}a_2$ can now be changed into $\mathrm{d}a^*_4 = \alpha^*_4\,\mathrm{d}\xi_4\,\mathrm{d}s$. Therefore, the relation $(8)_3$ for $\boldsymbol{f}_{2\Gamma}$ and the one for $\boldsymbol{c}_{2\Gamma}$ should now be refined into

$$\begin{aligned}
&\int\int_{\Pi^+_{2d}} \mathbf{t}^{*+}_2\,\mathrm{d}a^+_2 - \int\int_{\Pi^-_{2d}} \mathbf{t}^{*-}_2\,\mathrm{d}a^-_2 = \int_\Gamma \boldsymbol{f}_{2\Gamma}\,\mathrm{d}s,\\
&\boldsymbol{f}_{2\Gamma} = \int_{-h^-_3}^0 \alpha^+_2\alpha^*_3\mathbf{t}^{*+}_2\,\mathrm{d}\xi_3 - \int_{-h^-_4}^0 \alpha^-_2\alpha^*_4\mathbf{t}^{*-}_2\,\mathrm{d}\xi_4,\\
&\boldsymbol{c}_{2\Gamma} = \int_{-h^-_3}^0 \alpha^+_2\alpha^*_3\boldsymbol{\zeta}^+_{2\Gamma}\times\mathbf{t}^{*+}_2\,\mathrm{d}\xi_3 - \int_{-h^-_4}^0 \alpha^-_2\alpha^*_4\boldsymbol{\zeta}^-_{2\Gamma}\times\mathbf{t}^{*-}_2\,\mathrm{d}\xi_4.
\end{aligned} \tag{35}$$

The total force $\mathbf{F}_3(\Pi_3)$ and total torque $\mathbf{T}_{o3}(\Pi_3)$ vectors for the self-intersecting shell as well as definitions of all the fields are exactly the same as for the branching shell given in (9) and (19), where ∂P_{1d} and ∂P_{2d} in (11) and (20) now mean the upper part of the enlarged tube boundaries belonging to ∂P_3.

Finally, applying analogous transformations as in the case of $\mathbf{F}_3(\Pi_3)$, for the total force vector $\mathbf{F}_4(\Pi_4)$ we obtain

$$\mathbf{F}_4(\Pi_4) = \int\int_{\Pi_4} \boldsymbol{f}_4\,\mathrm{d}a_4 + \int_{\partial\Pi_4\setminus\partial M_f} \boldsymbol{n}_{4\nu}\,\mathrm{d}s + \int_{\partial\Pi_4\cap\partial M_f} \boldsymbol{n}^*_4\,\mathrm{d}s - \int_\Gamma \boldsymbol{f}_{4\Gamma}\,\mathrm{d}s - (\boldsymbol{n}_{4e} - \boldsymbol{n}_{4i}), \tag{36}$$

where

$$\boldsymbol{f}_4 = \int_{-h_4^-}^{+h_4^+} \mathbf{f}_4 \mu_4 \,\mathrm{d}\xi_4 + \alpha_4^+ \mathbf{t}_4^{*+} - \alpha_4^- \mathbf{t}_4^{*-},$$
$$\boldsymbol{n}_{4v} = \int_{-h_4^-}^{+h_4^+} \alpha_4^* \mathbf{t}_{4n} \,\mathrm{d}\xi_4, \quad \boldsymbol{n}_4^* = \int_{-h_4^-}^{+h_4^+} \alpha_4^* \mathbf{t}_4^* \,\mathrm{d}\xi_4. \tag{37}$$

Again, the correcting force $\boldsymbol{f}_{4\Gamma}$ in (36) should take into account the fictitious tractions $\mathbf{t}_4^{*\pm}$ applied on $\Pi_{4d}^{\pm}$ and included in definition $(37)_1$ of $\boldsymbol{f}_4$. The area elements of $\Pi_{4d}^{\pm}$ are $\mathrm{d}a_4^{\pm} = \alpha_4^{\pm}\mathrm{d}a_4$, where $\mathrm{d}a_4 = \mathrm{d}a_1^* = \alpha_1^*\mathrm{d}\xi_1\,\mathrm{d}s$ for Π_{4d}^+ and $\mathrm{d}a_4 = \mathrm{d}a_2^* = \alpha_2^*\mathrm{d}\xi_2\,\mathrm{d}s$ for Π_{4d}^-. In order to account in $\boldsymbol{f}_{4\Gamma}$ the volume force field $\mathbf{f}_4$ applied within the lower part of the tubes P_{1d} and P_{2d}, let us note that the elementary volume force is here $\mathbf{f}_4\,\mathrm{d}v_4 = \mathbf{f}_4\mu_4\,\mathrm{d}\xi_4\,\mathrm{d}a_4$, where $\mathrm{d}a_4 = \mathrm{d}a_1^* = \alpha_1^*\,\mathrm{d}\xi_1\,\mathrm{d}s$ when integrating over ∂P_{1d} and $\mathrm{d}a_4 = \mathrm{d}a_2^* = \alpha_2^*\,\mathrm{d}\xi_2\,\mathrm{d}s$ when integrating over ∂P_{2d}. As a result, we have

$$\boldsymbol{f}_{4\Gamma} = \int_{-h_1^-}^{0} \alpha_4^+\alpha_1^*\mathbf{t}_4^{*+}\,\mathrm{d}\xi_1 - \int_{-h_2^-}^{0} \alpha_4^-\alpha_2^*\mathbf{t}_4^{*-}\,\mathrm{d}\xi_2 + \int_{-h_1^-}^{0}\left(\int_0^{+h_4^+} \mathbf{f}_4\mu_4\,\mathrm{d}\xi_4\right)\alpha_1^*\,\mathrm{d}\xi_1$$
$$+ \int_{-h_2^-}^{0}\left(\int_{-h_4^-}^{0} \mathbf{f}_4\mu_4\,\mathrm{d}\xi_4\right)\alpha_2^*\,\mathrm{d}\xi_2. \tag{38}$$

Applying similar arguments as those leading to (12), the concentrated forces $\boldsymbol{n}_{4i}$ or $\boldsymbol{n}_{4i}^*$ acting at x_i read

$$\boldsymbol{n}_{4i} = \int\int_{(\partial P_{1d}\cup\partial P_{2d})\setminus\partial B_f^*} \mathbf{t}_{4n}\,\mathrm{d}a_4^*, \quad \boldsymbol{n}_{4i}^* = \int\int_{(\partial P_{1d}\cup\partial P_{2d})\cap\partial B_f^*} \mathbf{t}_4^*\,\mathrm{d}a_4^*, \tag{39}$$

where now $\partial P_{1d}\cup\partial P_{2d}$ mean the lower parts of boundaries belonging to ∂P_4 at x_i. The concentrated forces $\boldsymbol{n}_{4e}$ or $\boldsymbol{n}_{4e}^*$ at x_e are defined similarly to (39).

Summing up the results of $\mathbf{F}_1$, $\mathbf{F}_2$, $\mathbf{F}_3$, $\mathbf{F}_4$ for the self-intersecting shell we obtain the same formal expression (13) as for the branching shell. However, now in (13) the fields $\boldsymbol{f}$, $\boldsymbol{n}_v$, $\boldsymbol{n}^*$, and $\boldsymbol{f}_\Gamma$ follow from all four parts of P, while the concentrated forces $\boldsymbol{n}_i$, $\boldsymbol{n}_e$ follow from combining the force vectors $\mathbf{F}_3$ and $\mathbf{F}_4$ alone.

It is now apparent that using similar approach as for $\mathbf{T}_{o3}(\Pi_3)$ for the total torque vector $\mathbf{T}_{o4}(\Pi_4)$ we obtain

$$\mathbf{T}_{o4}(\Pi_4) = \int\int_{\Pi_4}(\boldsymbol{c}_4 + \boldsymbol{y}_4\times\boldsymbol{f}_4)\,\mathrm{d}a_4 + \int_{\partial\Pi_4\setminus\partial M_f}(\boldsymbol{m}_{4v} + \boldsymbol{y}_4\times\boldsymbol{n}_{4v})\,\mathrm{d}s + \int_{\partial\Pi_4\cap\partial M_f}(\boldsymbol{m}_4^* + \boldsymbol{y}_4\times\boldsymbol{n}_4^*)\,\mathrm{d}s$$
$$- \int_\Gamma(\boldsymbol{c}_{4\Gamma} + \boldsymbol{y}_\Gamma\times\boldsymbol{f}_{4\Gamma})\,\mathrm{d}s - \{(\boldsymbol{m}_{4e} + \boldsymbol{y}_{\Gamma e}\times\boldsymbol{n}_{4e}) - (\boldsymbol{m}_{4i} + \boldsymbol{y}_{\Gamma i}\times\boldsymbol{n}_{4i})\}, \tag{40}$$

where all 2D and 1D fields are defined analogously as in (17). Only for the correcting couples we have analogues of (38) and (39) in the form

$$\boldsymbol{c}_{4\Gamma} = \int_{-h_1^-}^{0}\alpha_4^+\alpha_1^*\boldsymbol{\zeta}_{4\Gamma}^+\times\mathbf{t}_4^{*+}\,\mathrm{d}\xi_1 - \int_{-h_2^-}^{0}\alpha_4^-\alpha_2^*\boldsymbol{\zeta}_{4\Gamma}^-\times\mathbf{t}_4^{*-}\,\mathrm{d}\xi_2$$
$$+ \int_{-h_1^-}^{0}\left(\int_0^{+h_4^+}\boldsymbol{\zeta}_\Gamma\times\mathbf{f}_4\mu_4\,\mathrm{d}\xi_4\right)\alpha_1^*\,\mathrm{d}\xi_1 + \int_{-h_2^-}^{0}\left(\int_{-h_4^-}^{0}\boldsymbol{\zeta}_\Gamma\times\mathbf{f}_4\mu_4\,\mathrm{d}\xi_4\right)\alpha_2^*\,\mathrm{d}\xi_2,$$
$$\boldsymbol{m}_{4i} = \int\int_{(\partial P_{1d}\cup\partial P_{2d})\setminus\partial B_f^*}\boldsymbol{\zeta}_\Gamma\times\mathbf{t}_{4n}\,\mathrm{d}a_4^*. \tag{41}$$

The concentrated couples $\boldsymbol{m}_{4i}^*$, $\boldsymbol{m}_{4e}$, and $\boldsymbol{m}_{4e}^*$ are defined accordingly.

Summing up the result of $\mathbf{T}_{o1}$, $\mathbf{T}_{o2}$, $\mathbf{T}_{o3}$, $\mathbf{T}_{o4}$ for the self-intersecting shell we obtain the same formal expression (21) as for the branching shell. However, now in (21) the fields $\boldsymbol{c}$, $\boldsymbol{m}_v$, $\boldsymbol{m}^*$, and $\boldsymbol{c}_\Gamma$ follow from all four parts of P, while $\boldsymbol{m}_i$, $\boldsymbol{m}_e$ are the result of combining the couples from $\mathbf{T}_{o3}$ and $\mathbf{T}_{o4}$.

The relations (13) and (21), with extended definitions of fields presented in this section, are again the exact 2D static equivalents for the self-intersecting shell of the global vectors $\mathbf{F}(P)$ and $\mathbf{T}_o(P)$ appearing in the 3D equilibrium conditions (3).

Further transformations of (13) and (21) in the case of the self-intersecting shell are exactly the same as those given in Section 4 for the branching shell, only now in definitions of jumps (26) we have to sum up over $k = 1, 2, 3, 4$. As a result, the global equilibrium conditions for the self-intersecting shell become formally identical to (28) and (29). Therefore, also the local dynamic conditions are the same as (30)–(33), only the fields present in the dynamic continuity conditions (32) and the dynamic boundary conditions (33) have to be calculated according to formulae derived in this section for the self-intersecting shell.

7. Discussion

We have discussed standard geometries of the junction region of the branching shell (Figs. 2(a), Fig. 3) and the self-intersecting shell (Figs. 4(a), Fig. 5). In more complex geometries of the junctions the reduction procedure should be understood as slightly modified.

As an example, let us assume the cross-section of the junction region of a quite general branching shell as is shown in Fig. 6(a). In this general case we can always introduce a base surface, for example starting Π_3 from the fold line of the lower shell face (see Fig. 6(b)) and then joining Π_1 and Π_2 along some Γ.

A detailed analysis of Fig. 6(b) and Fig. 3 indicates that in both cases we have similar extended surface strips Π^+_{1d}, Π^+_{2d}, Π^-_{3d}, Π^+_{3d} with fictitious tractions and tubes ∂P_{1d}, ∂P_{2d} of double integration. However, in Fig. 6(b) the skew thickness co-ordinate ξ_3 measures distance from Π_3 along two straight lines which are *different* above and below Π_3. The boundary surface ∂P_3 within the junction region consists now of two *different* rectilinear surfaces joined along the common surface curve Γ. Therefore, the formulae (10) should now be understood as being calculated segment-wise along the thickness co-ordinate ξ_3, which is now different above and below Π_3.

In Section 3 three regular parts of the branching shell structure have first been extended into the junction region up to Γ and then the surplus of additional resultant forces and couples has been *subtracted* along Γ. One might apply another statically equivalent approach as well: cut off first the junction region itself, then reduce forces applied in regular shell parts P_k to their static equivalents on Π_k, and finally *add* along Γ static equivalents of forces acting in the junction region. However, definition of such a junction region itself is not unique and different possible definitions would lead to different values of equivalent forces and couples along Γ. In such an approach the resultant forces and couples of the regular shell parts would be defined only up to some distance from Γ depending on the size of the defined junction region. As a result, we feel that such an approach, as not uniquely defined, would be less convenient in 2D modelling and analysis of branching and/or self-intersecting shells. Our reduction procedure described in Section 3 does not require of defining the junction region and, therefore, is independent of its definition.

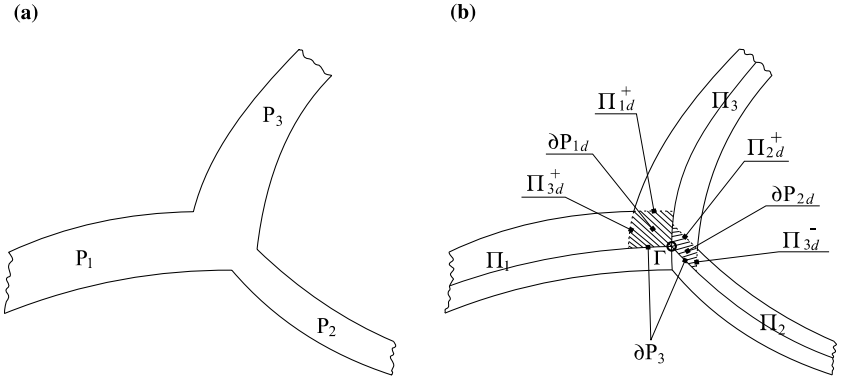

Fig. 6. Cross-section of the general branching shell: (a) the 3D shell, and (b) extended strips with fictitious tractions and tubes of double integration.

8. Conclusions

We have derived the exact, resultant, global and local equilibrium conditions for the non-linear theory of branching and self-intersecting shells. The conditions have been written on the reference base surface consisting of three (in case of branching) and four (in case of self-intersection) regular surfaces joined together along the common singular curve modelling the junction. The exact 2D equilibrium conditions have been formulated by performing direct through-the-thickness integration in the 3D global equilibrium conditions of continuum mechanics.

At regular surface and boundary points our local, resultant equilibrium equations and dynamic boundary conditions are equivalent to the ones published earlier. However, our resultant dynamic continuity conditions (32) along the singular curve Γ and dynamic boundary conditions (33) at singular boundary points x_i, x_e are new.

In the derivation process we have used no simplifying assumptions of any kind, apart of usual regularity requirements for the fields allowing all mathematical operations to be performed. Therefore, our results are valid for an arbitrary shell thickness which can be uniquely defined along the transverse co-ordinate ξ. They are applicable for an arbitrary internal through-the-thickness shell structure including layers, reinforcements, a mixture of several constituents, voids, cracks and other structural defects, provided that the internal 3D stress field is still integrable across the shell thickness. The results are also valid for an arbitrary material behaviour as well as for unrestricted values of translations, rotations, strains, and/or bendings of the shell material elements.

Applying a similar approach with appropriate modifications the exact, resultant dynamic continuity conditions for other types of shell irregularity can also be formulated. The structure of the conditions should be similar to the one of (32), only for each type of shell irregularity the fields $\boldsymbol{n}$, $\boldsymbol{m}$, $\boldsymbol{f}_\Gamma$, $\boldsymbol{c}_\Gamma$ would be defined by somewhat different expressions.

The additional 2D resultant equilibrium conditions derived here allow one to formulate the complete boundary value problem for the branching and self-intersecting shells. One only needs to appropriately refine the procedure leading to the six-field non-linear theory of irregular shells presented in Chróścielewski et al. (2004).

Acknowledgements

This research was supported by the Polish State Committee for Scientific Research under grant KBN No. 5 T07A 008 25.

Appendix A. Relations for differential elements

In the paper we frequently need to express differential volume elements as well as differential surface elements of the upper M^+ and lower M^- shell faces and of the shell lateral boundary surface ∂B^* through corresponding differential elements of M and ∂M.

Let any $\mathbf{x} \in B$ be parameterized by the co-ordinates $(\xi^\alpha,\xi) \equiv (\xi^i)$, $\alpha = 1,2$, $i = 1,2,3$, where ξ is the rectilinear co-ordinate measuring distance along the line defined by the unit vector $\boldsymbol{t}$ not necessarily normal to M, and ξ^α are Gaussian co-ordinates of M (Fig. A.1). The covariant $\boldsymbol{a}_\alpha$ and the contravariant $\boldsymbol{a}^\beta$ base vectors as well as the corresponding components $a_{\alpha\beta}$ and $a^{\alpha\beta}$ of the surface metric tensor of M are given by (see Fig. A.1)

$$\begin{aligned}
&\boldsymbol{a}_\alpha = \boldsymbol{P}\frac{\partial \boldsymbol{x}}{\partial \xi^\alpha} \equiv \boldsymbol{P}\boldsymbol{x}_{,\alpha}, \quad a_{\alpha\beta} = \boldsymbol{a}_\alpha \cdot \boldsymbol{a}_\beta, \quad a = \det(a_{\alpha\beta}),\\
&\boldsymbol{a}^\beta \cdot \boldsymbol{a}_\alpha = \delta^\beta_\alpha, \quad a^{\alpha\beta} = \boldsymbol{a}^\alpha \cdot \boldsymbol{a}^\beta, \quad \boldsymbol{n} = \frac{1}{2}\epsilon^{\alpha\beta}\boldsymbol{x}_{,\alpha} \times \boldsymbol{x}_{,\beta},\\
&\epsilon^{\alpha\beta} = \sqrt{a}e_{\alpha\beta}, \quad \epsilon^{\alpha\beta} = a^{\alpha\lambda}a^{\beta\mu}\epsilon_{\lambda\mu} = \frac{1}{\sqrt{a}}\epsilon^{\alpha\beta},
\end{aligned} \tag{A.1}$$

where $\boldsymbol{P}$ is the projection operator of M (see Gurtin and Murdoch, 1975), $\boldsymbol{n}$ is the unit normal vector orienting M, δ^β_α is the 2D Kronecker symbol such that $\delta^1_1 = \delta^2_2 = 1$, $\delta^2_1 = \delta^1_2 = 0$, while $e^{\alpha\beta} \equiv e_{\alpha\beta}$ are the surface permutation symbols such that $e_{11} = e_{22} = 0$, $e_{12} = -e_{21} = 1$.

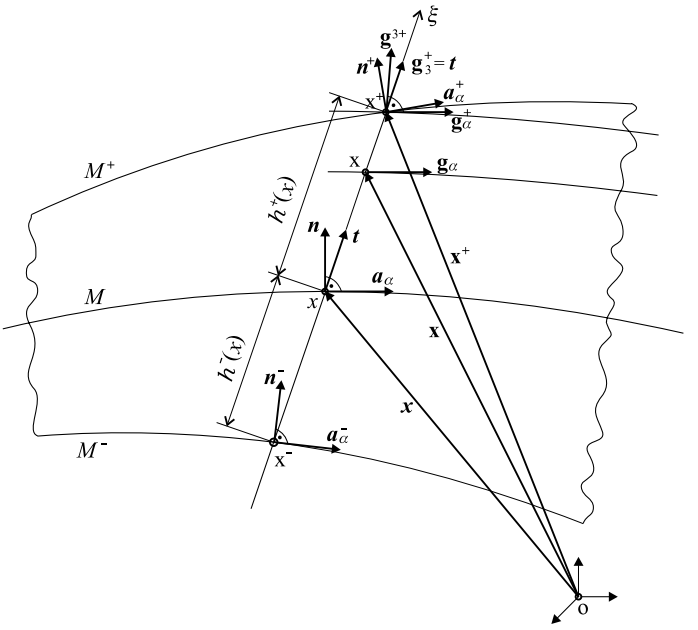

Fig. A.1. Shell geometry.

At any spatial point $\mathrm{x} \in B$ we have the following 3D relations analogous to those of (A.1):

$$\begin{aligned}
&\mathbf{g}_i = \mathbf{x}_{,i}, \quad g_{ij} = \mathbf{g}_i \cdot \mathbf{g}_j, \quad g = \det(g_{ij}),\\
&\mathbf{g}^j \cdot \mathbf{g}_i = \delta_i^j, \quad g^{ij} = \mathbf{g}^i \cdot \mathbf{g}^j, \quad \mathbf{g}^i = \frac{1}{2}\epsilon^{ijk}\mathbf{g}_j \times \mathbf{g}_k,\\
&\epsilon^{ijk} = \frac{1}{\sqrt{g}}e^{ijk}, \quad \epsilon_{ijk} = (\mathbf{g}_i \times \mathbf{g}_j) \cdot \mathbf{g}_k = \sqrt{g}e_{ijk},
\end{aligned} \tag{A.2}$$

where $\mathbf{g}_i$ and $\mathbf{g}^j$ are the spatial covariant and contravariant base vectors, while g_{ij} and g^{ij} are covariant and contravariant components of the metric tensor of $\mathscr{E}$, respectively. In (A.2), $e^{ijk} \equiv e_{ijk}$ are the 3D permutation symbols such that $e_{123} = e_{312} = e_{231} = -e_{132} = -e_{213} = -e_{321} = 1$, otherwise $e_{ijk} = 0$, while for the 3D Kronecker symbols $\delta_1^1 = \delta_2^2 = \delta_3^3 = 1$ and $\delta_i^j = 0$ for $i \neq j$.

The differential volume element $\mathrm{d}v$ of B and the differential surface element $\mathrm{d}a$ of M are defined by

$$\begin{aligned}
&\mathrm{d}v = \sqrt{g}\,\mathrm{d}\xi^1\,\mathrm{d}\xi^2\,\mathrm{d}\xi = \mu\,\mathrm{d}\xi\,\mathrm{d}a,\\
&\mathrm{d}a = \sqrt{a}\,\mathrm{d}\xi^1\,\mathrm{d}\xi^2, \quad \mu = \sqrt{\frac{g}{a}}.
\end{aligned} \tag{A.3}$$

The spatial base vectors $\mathbf{g}_i$ and $\mathbf{g}^j$ are expressed through the vectors $\boldsymbol{x}_{,\alpha}$ and $\boldsymbol{t}$ defined on M by the relations (Fig. A.1)

$$\begin{aligned}
&\mathbf{g}_\alpha = \boldsymbol{x}_{,\alpha} + \xi\boldsymbol{t}_{,\alpha}, \quad \mathbf{g}_3 = \boldsymbol{t},\\
&\mathbf{g}^\beta = \frac{1}{2}\epsilon^{ij\beta}\mathbf{g}_i \times \mathbf{g}_j = \mu^{-1}\epsilon^{\alpha\beta}\boldsymbol{t} \times \mathbf{g}_\alpha,\\
&\mathbf{g}^3 = \frac{1}{2}\epsilon^{3jk}\mathbf{g}_j \times \mathbf{g}_k = \frac{1}{2}\mu^{-1}\epsilon^{\alpha\beta}\mathbf{g}_\alpha \times \mathbf{g}_\beta,\\
&\mu = \frac{1}{2}\epsilon^{\alpha\beta}(\mathbf{g}_\alpha \times \mathbf{g}_\beta) \cdot \mathbf{g}_3 = \boldsymbol{n} \cdot \boldsymbol{t} + \xi\epsilon^{\alpha\beta}(\boldsymbol{x}_{,\alpha} \times \boldsymbol{t}_{,\beta}) \cdot \boldsymbol{t} + \frac{1}{2}\xi^2\epsilon^{\alpha\beta}(\boldsymbol{t}_{,\alpha} \times \boldsymbol{t}_{,\beta}) \cdot \boldsymbol{t}.
\end{aligned} \tag{A.4}$$

It follows from (1) that the position vector of the upper shell face M^+ and the base vectors on M^+ are (Fig. A.1)

$$\begin{aligned}&\mathbf{x}^+(\xi^\alpha)=\boldsymbol{x}(\xi^\alpha)+h^+(\xi^\alpha)\boldsymbol{t},\quad \boldsymbol{a}^+_\alpha=\boldsymbol{P}^+\mathbf{x}^+_{,\alpha},\\&\mathbf{x}^+_{,\alpha}=\mathbf{g}^+_\alpha+h^+_{,\alpha}\boldsymbol{t},\quad \mathbf{g}^+_\alpha=\mathbf{g}_\alpha|_{\xi=h^+}=\boldsymbol{x}_{,\alpha}+h^+\boldsymbol{t}_{,\alpha},\end{aligned}\tag{A.5}$$

where $\mathbf{g}^+_\alpha$ are the spatial base vectors at x^+ of the surface parallel to M at the distance $\xi=h^+$ measured along $\boldsymbol{t}$.

The differential surface element $\mathrm{d}a^+$ of M^+ can be defined through the vector identity

$$\mathrm{d}\boldsymbol{a}^+=\boldsymbol{n}^+\,\mathrm{d}a^+=\mathbf{x}^+_{,1}\times\mathbf{x}^+_{,2}\,\mathrm{d}\xi^1\,\mathrm{d}\xi^2.\tag{A.6}$$

Introducing (A.5)$_2$ into (A.6) we perform the following transformations:

$$\begin{aligned}\mathrm{d}\boldsymbol{a}^+&=(\mathbf{g}^+_1+h^+_{,1}\boldsymbol{t})\times(\mathbf{g}^+_2+h^+_{,2}\boldsymbol{t})\,\mathrm{d}\xi^1\,\mathrm{d}\xi^2=\sqrt{g^+}\mathbf{g}^{3+}\,\mathrm{d}\xi^1\,\mathrm{d}\xi^2+(h^+_{,1}\boldsymbol{t}\times\mathbf{g}^+_2-h^+_{,2}\boldsymbol{t}\times\mathbf{g}^+_1)\,\mathrm{d}\xi^1\,\mathrm{d}\xi^2\\&=\sqrt{\frac{g^+}{a}}\mathbf{g}^{3+}\,\mathrm{d}a+h^+_{,\alpha}\epsilon^{\alpha\beta}\boldsymbol{t}\times\mathbf{g}^+_\beta\,\mathrm{d}a=(\mathbf{g}^{3+}-h^+_{,\alpha}\mathbf{g}^{\alpha+})\mu^+\,\mathrm{d}a.\end{aligned}\tag{A.7}$$

It is easy to see from (A.6) and (A.7) that

$$\begin{aligned}|\mathrm{d}\boldsymbol{a}^+|&=|\boldsymbol{n}^+\,\mathrm{d}a^+|=+\sqrt{\boldsymbol{n}^+\cdot\boldsymbol{n}^+}\,\mathrm{d}a^+=\mathrm{d}a^+=\sqrt{(\mathbf{g}^{3+}-h^+_{,\alpha}\mathbf{g}^{\alpha+})\cdot(\mathbf{g}^{3+}-h^+_{,\beta}\mathbf{g}^{\beta+})}\mu^+\,\mathrm{d}a\\&=\sqrt{g^{33}-2h^+_{,\alpha}g^{\alpha3+}+h^+_{,\alpha}h^+_{,\beta}g^{\alpha\beta+}}\mu^+\,\mathrm{d}a.\end{aligned}\tag{A.8}$$

The position vector of the lower shell face M^- and its base vectors are (Fig. A.1)

$$\begin{aligned}&\mathbf{x}^-(\xi^\alpha)=\boldsymbol{x}(\xi^\alpha)-h^-(\xi^\alpha)\boldsymbol{t},\quad \boldsymbol{a}^-_\alpha=\boldsymbol{P}^-\mathbf{x}^-_{,\alpha},\\&\mathbf{x}^-_{,\alpha}=\mathbf{g}^-_\alpha-h^-_{,\alpha}\boldsymbol{t},\quad \mathbf{g}^-_\alpha=\mathbf{g}_\alpha|_{\xi=h^-}=\boldsymbol{x}_{,\alpha}-h^-\boldsymbol{t}_{,\alpha},\end{aligned}\tag{A.9}$$

where $\mathbf{g}^-_\alpha$ are the spatial base vectors at x^- for $\xi=-h^-$.

The differential surface element $\mathrm{d}a^-$ of M^- can again be defined through the vector identity

$$\mathrm{d}\boldsymbol{a}^-=-\boldsymbol{n}^-\,\mathrm{d}a^-=-\mathbf{x}^-_{,1}\times\mathbf{x}^-_{,2}\,\mathrm{d}\xi^1\,\mathrm{d}\xi^2,\tag{A.10}$$

where the minus sign in front of $\boldsymbol{n}^-$ follows conventionally from the requirement that $\mathrm{d}\boldsymbol{a}^-$ should point out in the outward direction to the lower shell face M^-.

Introducing (A.9)$_2$ into (A.10) and performing transformations analogous to (A.7) and (A.8) we obtain

$$|\mathrm{d}\boldsymbol{a}^-|=\mathrm{d}a^-=\sqrt{g^{33-}+2h^-_{,\alpha}g^{\alpha3-}+h^-_{,\alpha}h^-_{,\beta}g^{\alpha\beta-}}\mu^-\,\mathrm{d}a.\tag{A.11}$$

It follows from (A.8) and (A.11) that

$$\begin{aligned}&\mathrm{d}a^\pm=\alpha^\pm\,\mathrm{d}a,\\&\alpha^\pm=\mu^\pm\sqrt{g^{33\pm}\mp2h^\pm_{,\alpha}g^{\alpha3\pm}+h^\pm_{,\alpha}h^\pm_{,\beta}g^{\alpha\beta\pm}}.\end{aligned}\tag{A.12}$$

The shell lateral boundary surface ∂B^* is rectilinear one formed by straight lines along the vector $\boldsymbol{t}$ at each point $x\in\partial M$ (Fig. A.2). The differential surface element $\mathrm{d}a^*$ of ∂B^* can again be defined through the vector identity

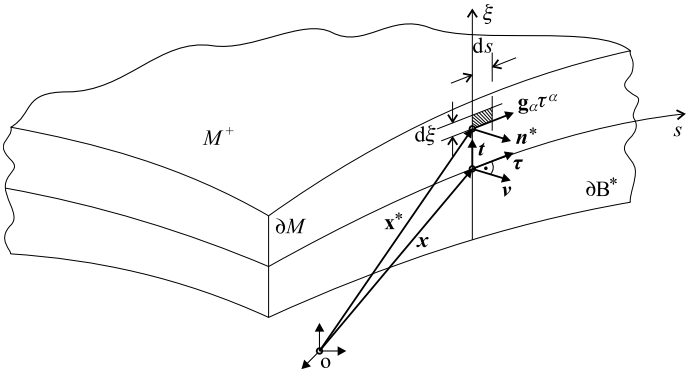

Fig. A.2. Geometry of the lateral boundary surface.

$$\mathrm{d}\boldsymbol{a}^* = \boldsymbol{n}^*\,\mathrm{d}a^* = \mathbf{x}^*_{,s}\times\mathbf{x}^*_{,\xi}\,\mathrm{d}s\,\mathrm{d}\xi = \mathbf{g}_\alpha\tau^\alpha\times\boldsymbol{t}\,\mathrm{d}s\,\mathrm{d}\xi = \epsilon_{\alpha3\beta}\mathbf{g}^\beta\tau^\alpha\,\mathrm{d}s\,\mathrm{d}\xi = \mathbf{g}^\beta v_\beta\mu\,\mathrm{d}s\,\mathrm{d}\xi, \tag{A.13}$$

so that

$$\mathrm{d}a^* = \alpha^*\,\mathrm{d}\xi\,\mathrm{d}s,\quad \alpha^* = \mu\sqrt{g^{\alpha\beta}v_\alpha v_\beta}. \tag{A.14}$$

In most shell problems we can take the transverse co-ordinate ξ to be orthogonal to M and, therefore, $\boldsymbol{t}\equiv\boldsymbol{n}$. Then, according to Pietraszkiewicz (1979),

$$\begin{aligned}
&\mathbf{g}_\alpha = \mu^\lambda_\alpha\boldsymbol{x}_{,\alpha},\quad \mathbf{g}^\beta = (\mu^{-1})^\beta_\lambda a^{\lambda\mu}\boldsymbol{x}_{,\mu},\quad \mathbf{g}_3 = \mathbf{g}^3 = n,\\
&\mu^\lambda_\alpha = \delta^\lambda_\alpha - \xi b^\lambda_\alpha,\quad \mu = \det(\mu^\lambda_\alpha) = 1 - 2\xi H + \xi^2 K,\\
&\mu^\lambda_\alpha(\mu^{-1})^\beta_\lambda = \delta^\beta_\alpha,\quad \mu^\lambda_\alpha(\mu^{-1})^\alpha_\mu = \delta^\lambda_\mu,\quad (\mu^{-1})^\beta_\lambda = \frac{1}{\mu}\{\delta^\beta_\lambda + \xi(b^\beta_\lambda - 2H\delta^\beta_\lambda)\},\\
&g_{\alpha\beta} = \mu^\lambda_\alpha\mu^\mu_\beta a_{\lambda\mu},\quad g^{\alpha\beta} = (\mu^{-1})^\alpha_\lambda(\mu^{-1})^\beta_\mu a^{\lambda\mu},\\
&g_{\alpha3} = g^{\alpha3} = 0,\quad g_{33} = g^{33} = 1,
\end{aligned} \tag{A.15}$$

where μ^λ_α and $(\mu^{-1})^\beta_\lambda$ are called shifters, and

$$\begin{aligned}
&b_{\alpha\beta} = -\boldsymbol{n}_{,\alpha}\cdot\boldsymbol{x}_{,\beta},\quad b^\lambda_\alpha = a^{\lambda\beta}b_{\alpha\beta},\quad b = \det(b_{\alpha\beta}),\\
&H = \frac{1}{2}b^\alpha_\alpha,\quad K = \frac{b}{a}.
\end{aligned} \tag{A.16}$$

In (A.16), $b_{\alpha\beta}$ and b^λ_α are covariant and mixed components of the curvature tensor, H is the mean curvature, and K is the Gaussian curvature of the reference base surface M.

In the normal co-ordinate system (ξ^α,ξ) the geometric expansion factors $\alpha^\pm$, α^* appearing in (A.12) and (A.14) can be simplified into

$$\alpha^\pm = \mu^\pm\sqrt{1 + h^\pm_{,\alpha}h^\pm_{,\beta}g^{\alpha\beta\pm}},\quad \alpha^* = \mu\sqrt{g^{\alpha\beta}v_\alpha v_\beta}, \tag{A.17}$$

where now μ and $g^{\alpha\beta}$ are given by (A.15).

If additionally the shell is of constant thickness and M is so chosen that h^+ and h^- do not depend on ξ^α, then $h^\pm_{,\alpha}\equiv 0$, and $\alpha^\pm = \mu^\pm$.

Appendix B. Supplementary data

Supplementary data associated with this article can be found, in the online version, at doi:10.1016/j.ijsolstr.2006.04.030.

References

Chróścielewski, J., Makowski, J., Stumpf, H., 1992. Genuinely resultant shell finite elements accounting for geometric and material non-linearity. International Journal for Numerical Methods in Engineering 35, 63–94.

Chróścielewski, J., Makowski, J., Stumpf, H., 1997. Finite element analysis of smooth, folded and multi-shell structures. Computer Methods in Applied Mechanics and Engineering 141, 1–46.

Chróścielewski, J., Makowski, J., Pietraszkiewicz, W., 2002. Non-linear dynamics of flexible shell structures. Computer Assisted Mechanics and Engineering Science 9, 341–357.

Chróścielewski, J., Makowski, J., Pietraszkiewicz, W., 2004. Statics and Dynamics of Multifold Shells: Nonlinear Theory and Finite Element Method (in Polish). Wydawnictwo IPPT PAN, Warszawa.

Eremeyev, V.A., Pietraszkiewicz, W., 2004. The non-linear theory of elastic shells with phase transitions. Journal of Elasticity 74, 67–86.

Gurtin, M.E., Murdoch, A.I., 1975. A continuum theory of elastic material surfaces. Archives for Rational Mechanics and Analysis 57, 291–323.

Libai, A., Simmonds, J.G., 1983. Nonlinear elastic shell theory. In: Hutchinson, J.W., Wu, T.Y. (Eds.), Advances in Applied Mechanics, vol. 23. Academic Press, New York, pp. 271–371.

Libai, A., Simmonds, J.G., 1998. The Nonlinear Theory of Elastic Shells, second ed. University Press, Cambridge.

Makowski, J., Stumpf, H., 1990. Buckling equations for elastic shells with rotational degrees of freedom undergoing finite strain deformation. International Journal of Solids and Structures 26, 353–368.

Makowski, J., Stumpf, H., 1994. Mechanics of Irregular Shell Structures. Institut für Mechanik, Ruhr-Universität, Mitteilung Nr. 95, Bochum, pp. 1–206.

Makowski, J., Pietraszkiewicz, W., Stumpf, H., 1999. Jump conditions in the non-linear theory of thin irregular shell. Journal of Elasticity 54, 1–26.

Pietraszkiewicz, W., 1979. Finite Rotations and Lagrangean Description in the Non-Linear Theory of Shells. Polish Sci. Publ., Warszawa-Poznań.

Pietraszkiewicz, W., 2001a. Nonlinear theories of shells (in Polish). In: Woźniak, C. (Ed.), Mechanics of Elastic Plates and Shells (in Polish). PWN, Warszawa, pp. 424–497.

Pietraszkiewicz, W., 2001b. On using rotations as primary variables in the non-linear theory of thin irregular shells. In: Durban, D. et al. (Eds.), Advances in the Mechanics of Plates and Shells. Kluwer, Amsterdam, pp. 245–258.

Pietraszkiewicz, W., Chróścielewski, J., Makowski, J., 2005. On dynamically and kinematically exact theory of shells. In: Pietraszkiewicz, W., Szymczak, Cz. (Eds.), Shell Structures: Theory and Applications. Taylor & Francis, London, pp. 163–167.

Reissner, E., 1974. Linear and nonlinear theory of shells. In: Fung, Y.C., Sechler, E.E. (Eds.), Thin Shell Structures. Prentice-Hall, Englewood Cliffs, pp. 29–44.

Reissner, E., 1982. A note on two-dimensional finite deformation theories of shells. International Journal of Non-Linear Mechanics 17 (3), 217–221.

Simmonds, J.G., 1984. The nonlinear thermodynamical theory of shells: Descent from 3-dimensions without thickness expansion. In: Axelrad, E., Emmerling, F. (Eds.), Flexible Shells. Springer-Verlag, Berlin, pp. 1–11.